Interaction Notes

Note 556

October 1999

An analytic study of the electric current on curved transmission line segments

Frank Gronwald and Jürgen Nitsch

Otto-von-Guericke-University Magdeburg
Institute for Fundamental Electrical Engineering and EMC
Post Box 4120
39016 Magdeburg
Germany

Abstract

We apply a recently established geometric expansion method to the construction of the electric current on a curved transmission line segment which is excited by a current wave. This construction involves an advanced thin wire approximation and a regularization of the Green's function that describes the current/current interaction on the wire. In particular, the damping of the exciting current wave at the bend can analytically be described.

1 Introduction

Within the framework of Electromagnetic Compatibility it is often necessary to analyze the coupling of electromagnetic fields into complex electric and electronic systems. This usually undesired coupling often takes place at transmission lines and can, in case of uniform, almost-uniform, or highly symmetric transmission lines, be described by (generalized) transmission line equations to obtain the dynamics of the electric current on the transmission line [1, 2]. For transmission lines which strongly deviate from uniformity and carry high frequency signals the assumptions of the (generalized) transmission line theory are usually no longer valid and one has to rely on the basic Maxwell theory. To obtain in this case analytical solutions for an actual problem is a mathematically demanding task which usually can only be solved in an approximative way.

We have recently proposed a general expansion method which is suitable to considerably reduce the mathematical effort in explicitly constructing the solution of Maxwell's equation for problems which involve arbitrarily curved transmission line structures [3]. The expansion has the physical meaning of a scattering expansion which yields low frequency corrections to the geometric theory of diffraction. The subject of this paper is the application of this method to the analysis of the current/current self-interaction of an excited curved wire segment which is due to its own electromagnetic radiation fields. We note that differential geometric methods in electrical engineering have already proven to be useful in the context of electromagnetic lens design [4].

The organization of the paper is as follows: In Sec. 2 we will review our expansion method which consists of a scattering expansion that can be simplified by a further geometric expansion. In Sec. 3 we will introduce the curved wire model considered and describe how the electric current on the wire can be explicitly constructed. The main steps of this construction are a thin wire approximation and a regularization procedure. Some conclusions are provided in Sec. 4.

2 A geometric scattering expansion

The geometric scattering expansion which is the basis of this study has been outlined in detail in [3]. In this section we will sketch the main steps of its derivation.

2.1 Derivation of a magnetic field integral equation

We start from the wave equation for the electromagnetic vector potential $\boldsymbol{A}$ in frequency domain with time dependence $\exp(-j\omega t) = \exp(-jkt/c)$,

$$\triangle \boldsymbol{A} + k^2 \boldsymbol{A} = -\mu \boldsymbol{J} \,, \qquad (1)$$

where the Lorentz gauge and SI units have been assumed. The retarded standard solution of this equation is

$$A(\boldsymbol{r}) = \mu \int G(\boldsymbol{r},\boldsymbol{r}')\boldsymbol{J}(\boldsymbol{r}')\, d^3r' , \tag{2}$$

with $G(\boldsymbol{r},\boldsymbol{r}') = \exp(jk|\boldsymbol{r}-\boldsymbol{r}'|)/4\pi|\boldsymbol{r}-\boldsymbol{r}'|$ the retarded Green's function of free space. The corresponding magnetic field is given by

$$\boldsymbol{H}(\boldsymbol{r}) = \nabla_r \times \int G(\boldsymbol{r},\boldsymbol{r}')\boldsymbol{J}(\boldsymbol{r}')\, d^3r' . \tag{3}$$

The coupling of the electromagnetic field to the transmission line current can be expressed by a boundary condition for the magnetic field on the surface of the transmission line. To this end we assume the transmission line to be a (fairly) good conductor and thus may assume the transmission line current $\boldsymbol{J}$ to be of the form of a surface current $\boldsymbol{k}$. Then the required boundary condition is given by

$$\boldsymbol{n} \times \boldsymbol{H} = \boldsymbol{k} \quad \text{(on the surface)} . \tag{4}$$

The current $\boldsymbol{k}$ is the sum of an (initially known) source current $\boldsymbol{k}_s$ and an (initially unknown) induced current $\boldsymbol{k}_c$ which is due to scattered electromagnetic fields, $\boldsymbol{k} = \boldsymbol{k}_s + \boldsymbol{k}_c$. In the same way we have the magnetic field as the sum of a primary field $\boldsymbol{H}_s$, which is due to $\boldsymbol{k}_s$, and an induced magnetic field $\boldsymbol{H}_c$, which is due to $\boldsymbol{k}_c$, that is, $\boldsymbol{H} = \boldsymbol{H}_s + \boldsymbol{H}_c$. With these splittings the boundary condition (4), together with (3), yields an integral equation for the determination of $\boldsymbol{k}_c$,

$$\boldsymbol{k}_c(\boldsymbol{r}) = \boldsymbol{n}_r \times \boldsymbol{H}_s - \boldsymbol{k}_s + \int \boldsymbol{n}_r \times \left[\nabla_r \times \left(G(\boldsymbol{r},\boldsymbol{r}')\boldsymbol{k}_c(\boldsymbol{r}')\right)\right] d^2\sigma' . \tag{5}$$

2.2 The scattering expansion

Let us define the current

$$\boldsymbol{k}_{1c} := \boldsymbol{n} \times \boldsymbol{H}_s - \boldsymbol{k}_s \tag{6}$$

and the functional

$$F ... := \int \boldsymbol{n}_r \times \left[\nabla_r \times \left(G(\boldsymbol{r},\boldsymbol{r}')...(\boldsymbol{r}')\right)\right] d^2\sigma' . \tag{7}$$

We write (5) in the form

$$\boldsymbol{k}_c(\boldsymbol{r}) = \boldsymbol{k}_{1c}(\boldsymbol{r}) + (F\boldsymbol{k}_c)(\boldsymbol{r}) , \tag{8}$$

and obtain by iteration

$$\begin{aligned} \boldsymbol{k}_c &= \boldsymbol{k}_{1c} + F\boldsymbol{k}_{1c} + F^2\boldsymbol{k}_{1c} + \cdots \\ &= \boldsymbol{k}_{1c} + \boldsymbol{k}_{2c} + \boldsymbol{k}_{3c} + \cdots \end{aligned} \tag{9}$$

with $\boldsymbol{k}_{(n+1)c} = F\boldsymbol{k}_{nc}$. It is straightforward to recognize that (9) constitutes a scattering expansion where the nth term $\boldsymbol{k}_{nc}$ accounts for contributions of electromagnetic fields which have been scattered $(n-1)$-times at the transmission line structure.

2.3 The geometric expansion

The scattering expansion (9) involves terms of the form $(F\boldsymbol{k}_{nc})(\boldsymbol{r})$ which have to be evaluated in order to construct the induced current $\boldsymbol{k}_{nc}$. But even for transmission lines of rather simple geometry this cannot be done in closed form.

An approximate evaluation can be performed if we observe that the surface integral $(F\boldsymbol{k}_{nc})(\boldsymbol{r})$ usually receives its main contribution from the vicinity of $\boldsymbol{r}$. It is then reasonable to expand its integrand around $\boldsymbol{r}$. To that end we introduce a coordinate system with its origin at $\boldsymbol{r}$, i.e., $\boldsymbol{r} = (0,0,0)$, in the following way [3, 5]: As x- and y-axis we take the principal axes of the surface at $\boldsymbol{r}$ with principal curvatures κ_1 and κ_2, respectively. Their orientation is chosen such that we obtain a right-handed coordinate system at $\boldsymbol{r}$ if the outwards pointing normal vector $\boldsymbol{n}_r$ is chosen as z-axis. Then a Taylor expansion of the third component of $\boldsymbol{r}' = (x', y', z')$ yields

$$z'(x',y') = \frac{1}{2}\Big(\kappa_1(\boldsymbol{r}')x'^2 + \kappa_2(\boldsymbol{r}')y'^2\Big) + \cdots . \tag{10}$$

The dots indicate terms of third and higher order in the distance $|\boldsymbol{r} - \boldsymbol{r}'| = |\boldsymbol{r}'| = r'$ and also contain derivatives of the principal curvatures. It is important to note that the scale of r' must be seen in relation to the principal curvatures, i.e., the expansion is a good approximation for $\kappa_1 r' \ll 1$ and $\kappa_2 r' \ll 1$.

With the expansion (10) it is possible to show that

$$(F\boldsymbol{k}_{nc})(\boldsymbol{r}) = \boldsymbol{k}_{(n+1)c}(\boldsymbol{r}) = \int \frac{G'(\boldsymbol{r},\boldsymbol{r}')}{r'} k_{nc}(\boldsymbol{r}')\Big(\kappa_1(\boldsymbol{r})\boldsymbol{v}^{\theta_n}(\boldsymbol{r}') + \kappa_2(\boldsymbol{r})\boldsymbol{w}^{\theta_n}(\boldsymbol{r}') + \cdots\Big)\, d^2\sigma' . \tag{11}$$

Here we defined $G'(\boldsymbol{r},\boldsymbol{r}') := \partial G(|\boldsymbol{r}-\boldsymbol{r}'|)/\partial(|\boldsymbol{r}-\boldsymbol{r}'|)$, $k_{nc}(\boldsymbol{r}') := |\boldsymbol{k}_{nc}(\boldsymbol{r}')|$, and the vectors

$$\boldsymbol{v}^{\theta_n}(\boldsymbol{r}') := \begin{pmatrix} x'^2(\sin\theta_n - \cos\theta_n) \\ x'^2(\sin\theta_n + \cos\theta_n) - 2x'y'(\sin\theta_n - \cos\theta_n) \\ 0 \end{pmatrix} , \tag{12}$$

$$\boldsymbol{w}^{\theta_n}(\boldsymbol{r}') := \begin{pmatrix} -y'^2(\sin\theta_n - \cos\theta_n) + 2x'y'(\sin\theta_n + \cos\theta_n) \\ -y'^2(\sin\theta_n + \cos\theta_n) \\ 0 \end{pmatrix} , \tag{13}$$

with θ_n the angle between the unit vector

$$\boldsymbol{e}_{r'} = \frac{1}{\sqrt{2}}(1, 1, \kappa_1 x' + \kappa_2 y') \tag{14}$$

at $\boldsymbol{r}'$ and the current vector $\boldsymbol{k}_{nc}(\boldsymbol{r}')$.

The result (11) is applicable to two-dimensional transmission line structures like the surface of a wire. However, it is often convenient to approximate such a structure by a one-dimensional line. In this case it is possible to derive the formula [3]

$$k_{(n+1)c}(\boldsymbol{r}) = a \int \frac{G'(\boldsymbol{r},\boldsymbol{r}')}{r'} k_{nc}(\boldsymbol{r}')\Big(\frac{\kappa y'^2}{2} + \frac{\kappa' y'^3}{3} + \cdots\Big) dy'. \tag{15}$$

Here the factor a is an (a priori undetermined) geometry factor which reflects the geometry of the (small) cross section of the line, y' parametrizes the line such that the tangent vector $\partial/\partial y'$ along the line is a unit vector, κ denotes the curvature of the line, and κ' denotes the derivative $\partial\kappa/\partial y'$. Of course, formulae (11) and (15) should be related by a thin wire approximation. That this is indeed the case will be shown in Sec. 3.2.

3 Application to a curved wire segment

3.1 The excited curved wire segment

We will focus in the following on a transmission line segment as shown in Fig. 1. The segment is assumed to be of the form of a curved wire which consists of two straight parts that are continuously connected by a circular arc of radius R. Its cross section is circular and of radius ρ. We parametrize the length of the wire by y. Furthermore we assume on the surface of the wire a source current of the form

$$\boldsymbol{k}_s = \boldsymbol{k}_0 \exp(jky)\,, \tag{16}$$

i.e., a current wave which travels towards increasing y. (Note that we assumed a time dependence $\exp(-j\omega t) = \exp(-jkt/c)$.)

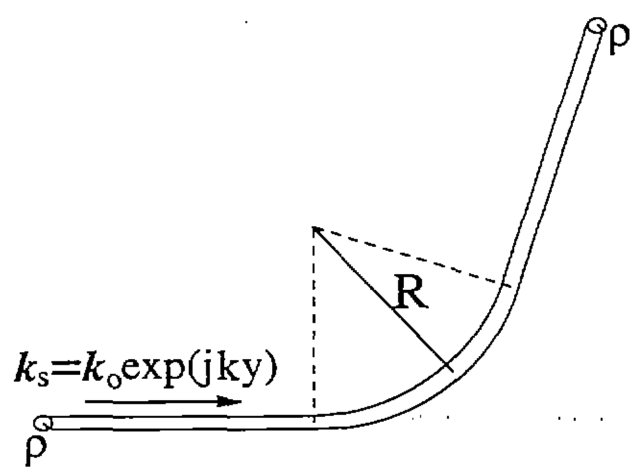

Fig. 1: A current wave travelling on a curved wire segment.

The problem consists in the determination of the induced current $\boldsymbol{k}_c$ on the wire which we expect as a consequence of the bend of the wire. Once $\boldsymbol{k}_c$ is constructed on the basis of Maxwell's theory the electromagnetic problem is solved.

3.2 Thin wire approximation

Though the main result (11) is applicable to currents on arbitrary surfaces, like the current on the surface of the curved wire segment, it is convenient to first perform a thin wire approximation in order to keep things relatively simple.

The geometry of the curved section of the wire can be described as part of a torus which is characterized by a central radius R and an internal radius ρ, as in Fig. 2.

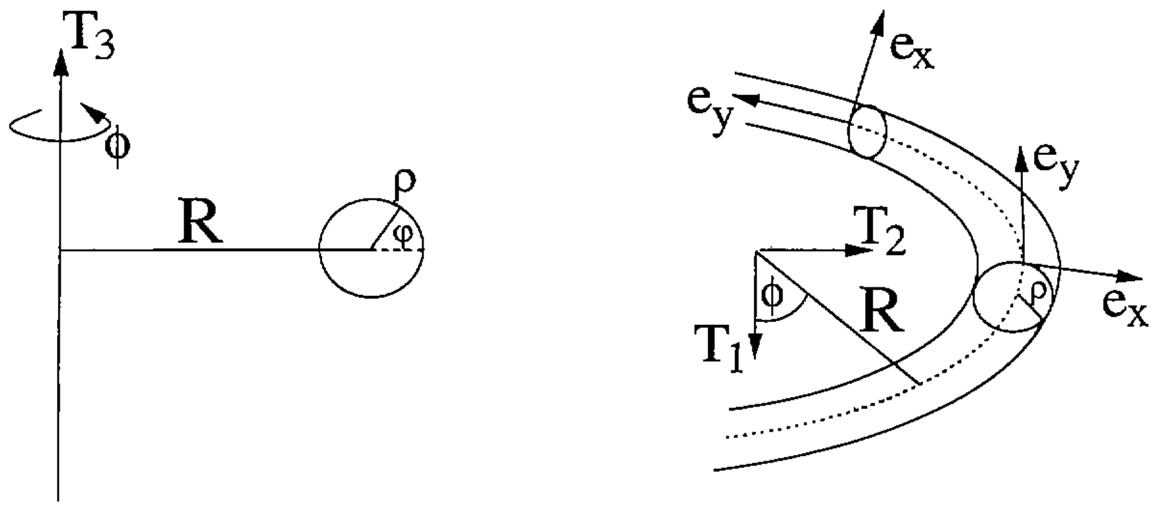

Fig. 2: The geometry of the curved section of the wire.

The surface of the torus, and thus the surface of the wire, is parametrized by two angles ϕ and φ. This is also indicated in Fig. 2. An explicit parametrization reads [5]

$$\begin{aligned} \boldsymbol{T}(\phi,\varphi) &= \Big(T_1(\phi,\varphi), T_2(\phi,\varphi), T_3(\phi,\varphi)\Big) \\ &= \Big((R+\rho\cos(\varphi))\cos(\phi), (R+\rho\sin(\varphi))\sin(\phi), \rho\sin(\varphi)\Big)\,, \end{aligned}$$

with the T_3-axis the axis of revolution and the T_1T_2-plane the symmetry plane of the torus. The angle φ ranges from 0 to 2π, the range of ϕ is from 0 to 2π for the full torus and, of course, smaller if only a curved section of the wire is considered.

From the parametrization (17) it is possible to derive the principal curvatures κ_1 and κ_2 of the torus and the curved wire segment. We first notice that at each point of the surface of the torus the two principal axes are tangent to the coordinate lines $\phi = \text{const}$ and $\varphi = \text{const}$. Let us take the principal curvature which corresponds to the coordinate line $\phi = \text{const}$ as κ_1 and κ_2 as corresponding to $\varphi = \text{const}$. Then it can be shown that

$$\kappa_1 = \frac{1}{\rho} = \text{const}\,, \quad \kappa_2 = \frac{\cos(\varphi)}{R+\rho\cos(\varphi)}\,. \tag{17}$$

The angle φ is measured as indicated in Fig. 3. Note that in particular we have

$$\kappa_2(\varphi = \pi/2) = \kappa_2(\varphi = 3\pi/2) = 0\,, \tag{18}$$

$$\kappa_2(\varphi = 0) = 1/(R+\rho)\,, \tag{19}$$

$$\kappa_2(\varphi = \pi) = -1/(R-\rho)\,, \tag{20}$$

as intuitively expected.

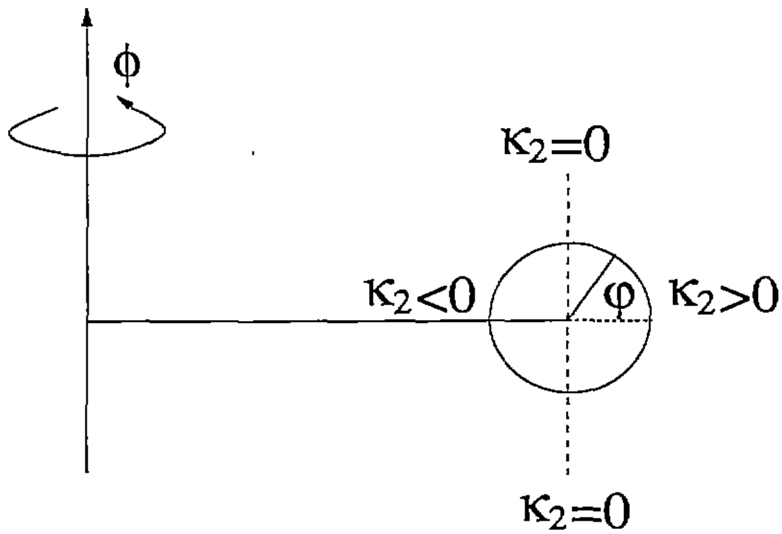

Fig. 3: In contrast to the principal curvature $\kappa_1 = 1/\rho$ of the torus the principal curvature κ_2 depends on the angle φ according to (17).

Now we introduce at each point of the surface of the curved wire segment an xyz-coordinate system as described in Sec. 2.3. An appropriate choice is determined by unit vectors

$$\boldsymbol{e}_x = -\frac{1}{\rho}\frac{\partial}{\partial\varphi}\,, \quad \boldsymbol{e}_y = \frac{1}{R+\rho\cos(\varphi)}\frac{\partial}{\partial\phi}\,, \quad \boldsymbol{e}_z = \boldsymbol{e}_x \times \boldsymbol{e}_y\,. \tag{21}$$

This means that $\boldsymbol{e}_x$ is tangent to the coordinate lines ϕ = const and oriented in the mathematically negative sense with respect to φ, $\boldsymbol{e}_y$ is tangent to the coordinate lines φ = const and oriented in the mathematically positive sense with respect to ϕ, and $\boldsymbol{e}_z$ is a normal vector on the surface which points outwards. For $\boldsymbol{e}_x$, $\boldsymbol{e}_y$ this convention is sketched on the right hand side of Fig. 2.

After these geometric preliminaries we are now in a position to apply the desired thin wire approximation to (11). Our assumptions are as follows:

1. At each point the current $\boldsymbol{k}$ and its single contributions are parallel to $\boldsymbol{e}_y$.
2. There is no current/current interaction transverse to $\boldsymbol{e}_y$. This means in particular that distances $|\boldsymbol{r} - \boldsymbol{r}'| = r'$, as they occur in (11), do not depend on φ.

3. The value of the current $\boldsymbol{k}$ and its single contributions do not vary with φ.

4. The radius R is considerably larger than ρ, i.e., $R \gg \rho$.

The first assumption implies that θ_n, as it appears in (12) and (13), assumes the value $\pi/4$ or $\pi/4+\pi$. The second assumption yields $x'=0$ in (12) and (13). Therefore we obtain

$$\boldsymbol{v}^{\theta_n}(\boldsymbol{r}') = 0\,, \qquad \boldsymbol{w}^{\theta_n}(\boldsymbol{r}') = \mp\frac{y'^2}{2}\boldsymbol{e}_y\,, \tag{22}$$

with the upper sign for $\theta_n = \pi/4$ and the lower sign for $\theta_n = \pi/4+\pi$. It follows that (11) reduces to

$$(F\boldsymbol{k}_{nc})(\boldsymbol{r}) = \mp\frac{1}{2}\int \frac{G'(\boldsymbol{r},\boldsymbol{r}')}{r'} k_{nc}(\boldsymbol{r}')\kappa_2(\boldsymbol{r}) y'^2 \boldsymbol{e}_y\, d^2\sigma'\,. \tag{23}$$

The volume element $d^2\sigma'$ explicitly reads

$$d^2\sigma' = dx'\,dy' = \rho\, d\varphi'\,dy'\,. \tag{24}$$

Clearly we wish to integrate out φ'. From the second and third assumption of the thin wire approximation we conclude that both $G'(\boldsymbol{r},\boldsymbol{r}')$ and k_{nc} do not depend on φ. Also, for geometric reasons, the Green's function $G'(\boldsymbol{r},\boldsymbol{r}')$ contributes to the integral only if both $\boldsymbol{r}$ and $\boldsymbol{r}'$ are within the region $\kappa_2 < 0$, i.e., within the region $\pi/2 < \varphi < 3\pi/2$. Otherwise the path determined by $\boldsymbol{r}-\boldsymbol{r}'$ intersects the curved wire segment and is forbidden for the freely propagating electromagnetic field. Therefore integration over φ involves the computation of the integral

$$\int_{\frac{\pi}{2}}^{\frac{3\pi}{2}} \kappa_2(\varphi)\,d\varphi = \int_{\frac{\pi}{2}}^{\frac{3\pi}{2}} \frac{\cos(\varphi)}{R+\rho\cos(\varphi)}\,d\varphi\,. \tag{25}$$

This integral can be solved analytically to yield

$$\int_{\frac{\pi}{2}}^{\frac{3\pi}{2}} \frac{\cos(\varphi)}{R+\rho\cos(\varphi)}\,d\varphi = \Big[-\frac{2R}{\rho\sqrt{R^2-\rho^2}}\arctan\Big(\frac{(R-\rho)\tan(\varphi/2)}{\sqrt{R^2-\rho^2}}\Big) + \frac{\varphi}{\rho}\Big]_{\frac{\pi}{2}}^{\frac{3\pi}{2}}\,.$$

However, for our purposes it is sufficient to take the condition $R \gg \rho \geq \rho\cos(\varphi)$ and compute (25) according to

$$\int_{\frac{\pi}{2}}^{\frac{3\pi}{2}} \frac{\cos(\varphi)}{R+\rho\cos(\varphi)}\,d\varphi \approx \int_{\frac{\pi}{2}}^{\frac{3\pi}{2}} \frac{\cos(\varphi)}{R}\,d\varphi = -\frac{2}{R}\,. \tag{26}$$

This yields

$$(F\boldsymbol{k}_{nc})(\boldsymbol{r}) = \pm\frac{\rho}{R}\int \frac{G'(\boldsymbol{r},\boldsymbol{r}')}{r'} k_{nc}(\boldsymbol{r}')\boldsymbol{e}_y\, y'^2\,dy'\,. \tag{27}$$

We define $\kappa := 1/R$, note the redundancy of $\boldsymbol{e}_y$, and finally obtain

$$k_{(n+1)c}(\boldsymbol{r}) = \pm\rho\kappa\int \frac{G'(\boldsymbol{r},\boldsymbol{r}')}{r'}\, k_{nc}(\boldsymbol{r}')y'^2\,dy'\,. \tag{28}$$

With $a = 2\rho$ we thus recover the lowest order term of formula (15) which was directly derived from a one-dimensional geometric formulation.

3.3 Determination of the first order induced current

Now that we have performed a thin wire approximation, we reconsider the curved wire segment of Fig. 1 which is modelled as a one-dimensional structure, compare Fig. 4. We still assume the wire to be excited by a current wave of the form (16). This current has to be understood as a zeroth order current that does not take into account the curved geometry of the wire segment.

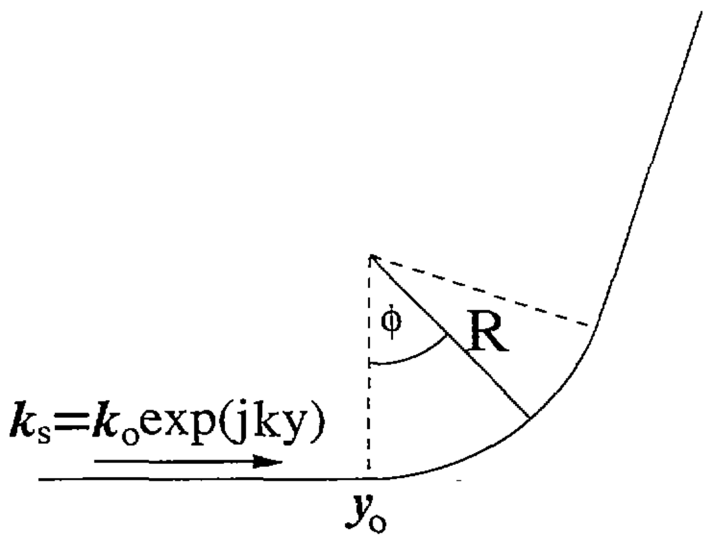

Fig. 4: The curved wire segment as reduced to a one-dimensional structure.

We now use the curvature expansion, i.e., in particular formula (28), to determine the induced current $\boldsymbol{k}_c$. We have

$$\boldsymbol{k} = \boldsymbol{k}_s + \boldsymbol{k}_{1c} + \boldsymbol{k}_{2c} + \dots \,, \tag{29}$$

with $\boldsymbol{k}_s$ explicitly given by (16). The first order induced current $\boldsymbol{k}_{1c}$ was defined in (6) as

$$\boldsymbol{k}_{1c} := \boldsymbol{n} \times \boldsymbol{H}_s - \boldsymbol{k}_s \,.$$

In our case it receives contributions from electromagnetic fields that are represented by $\boldsymbol{H}_s$ and generated by $\boldsymbol{k}_s$. More precisely, if $\boldsymbol{r}$ is a point on the wire the current $\boldsymbol{k}_{1c}(\boldsymbol{r})$ is induced by the magnetic field $\boldsymbol{H}_s^{\boldsymbol{r}\neq\boldsymbol{r}'}$ which is the sum of the magnetic fields at $\boldsymbol{r}$ that are generated by $\boldsymbol{k}_s(\boldsymbol{r}')$ for all $\boldsymbol{r}' \neq \boldsymbol{r}$. That $\boldsymbol{k}_s(\boldsymbol{r})$ does not contribute to $\boldsymbol{k}_{1c}(\boldsymbol{r})$ but is compensated by the outgoing field $\boldsymbol{H}_s^{\boldsymbol{r}=\boldsymbol{r}'}$ is deduced from the observation that there is no induced current $\boldsymbol{k}_c$ if the wire is straight. In this case the boundary condition (4) reduces to

$$0 = \boldsymbol{n}_r \times \boldsymbol{H}_s^{\boldsymbol{r}=\boldsymbol{r}'}(\boldsymbol{r}) - \boldsymbol{k}_s(\boldsymbol{r}) \,. \tag{30}$$

Therefore we obtain

$$\boldsymbol{k}_{1c}(\boldsymbol{r}) = \boldsymbol{n} \times \boldsymbol{H}_s^{r \neq r'}(\boldsymbol{r}) = \int_{r \neq r'} \boldsymbol{n}_r \times \left[\boldsymbol{\nabla}_r \times \left(G(\boldsymbol{r}, \boldsymbol{r}') \boldsymbol{k}_s(\boldsymbol{r}') \right) \right] d^2\sigma' . \tag{31}$$

Within the approximation provided by the curvature expansion the last term can immediately be rewritten by means of the result (28) to yield

$$k_{1c}(\boldsymbol{r}) = \rho\kappa \int \frac{G'(\boldsymbol{r}, \boldsymbol{r}')}{r'} k_s(\boldsymbol{r}') y'^2 \, dy' , \tag{32}$$

where we have used $\theta_s = \pi/4$ and thus chosen the positive sign. According to Fig. 4 the points on the curved section of the wire segment can be parametrized by $y = y_0 + R\phi$. We note that the corresponding tangent vector $\partial/\partial y = \partial/R\partial\phi$ is normalized to unity such that $y - y_0$ is a measure for the length of the arc between y and y_0. Thus we have in (32), to first order, $|y'| \approx r'$ and obtain

$$k_{1c}(\boldsymbol{r}) = \rho\kappa \int G'(\boldsymbol{r}, \boldsymbol{r}') \, k_s(\boldsymbol{r}') |y'| \, dy' . \tag{33}$$

This is already a very compact formula. The Green's function reads explicitly

$$G(\boldsymbol{r}, \boldsymbol{r}') = G(|\boldsymbol{r} - \boldsymbol{r}'|) \approx G(|y'|) = \frac{\exp(jk|y'|)}{4\pi|y'|} , \tag{34}$$

and its derivative is

$$G'(|y'|) = \frac{\partial G(|y'|)}{\partial |y'|} = jk \frac{\exp(jk|y'|)}{4\pi|y'|} - \frac{\exp(jk|y'|)}{4\pi|y'|^2} . \tag{35}$$

With the ansatz (16) the integrand of (33) becomes

$$\begin{aligned} G'(|y'|) \, k_s(y')|y'| = & -\frac{k_0}{4\pi}\left(k \sin(k(|y'| + y')) + \frac{\cos(k(|y'| + y'))}{|y'|} \right) \\ & + j\frac{k_0}{4\pi}\left(k \cos(k(|y'| + y')) - \frac{\sin(k(|y'| + y'))}{|y'|} \right) , \end{aligned} \tag{36}$$

where we have separated the real and imaginary parts.

3.4 Regularization of the Green's function

The real part of (36) exhibits a singularity at $|y'| = 0$ where it diverges proportionally to $1/y'$. This divergence is due to the singular behavior of $G(\boldsymbol{r}, \boldsymbol{r}')$ for $\boldsymbol{r}' \to \boldsymbol{r}$. However, it is not a physically meaningful divergence: In the limit $k \to 0$, i.e., the low-frequency limit, the induced current $\boldsymbol{k}_c$ should vanish since in this case the electromagnetic field becomes static. This is not in accordance with the recursion formula (33) where in the limit $k \to 0$ we end up with a diverging integral that contains a $1/|y'|$ singularity at $|y'| = 0$. It is thus obvious that our formalism does not work in the low frequency limit.

The reason for this failure is rooted in our ansatz: The derivation of the scattering expansion is based on the boundary condition (4) which, in turn, is based on the notion of a surface current and a sufficiently quick decay of the magnetic field within the conductor. This assumption is reasonable for sufficiently high frequencies but no longer fulfilled in the limit $k \to 0$. Therefore we have to eliminate the quasistatic contributions which make $\boldsymbol{k}_c$ diverge. One of the following two regularization schemes can be used for this purpose.

1. *"Subtraction scheme":* We define a regularized function $G'_{\text{reg}} = G' - f_{\text{reg}}$ where f_{reg} has the same singular behavior as G'. Conceivable choices are of the form $f_{\text{reg}} = \exp(-\gamma|y'|)/|y'|$. The parameter γ must be chosen such that in regions of $|y'|$ which do not correspond to the quasistatic regime f_{reg} is small compared to G'_{reg}. That is, a large value of γ, for example, can make f_{reg} small even for small $|y'|$. However, for *all* values of γ the singular behavior of G' gets subtracted out.
2. *"Cut-off scheme":* We introduce a cut-off parameter ε and demand $|y'| > \varepsilon$ such that smaller values of $|y'|$ which do correspond to the quasistatic regime are not integrated over.

Both schemes introduce a free parameter (γ or ε), the value of which is a priori not fixed but characterized by a certain length scale ℓ. The length scale ℓ is the one at which, for a given frequency f, the electromagnetic field appears to be quasistatic. It is connected to the decay length of time harmonic electromagnetic fields in a conductor and can be estimated from a diffusion equation for the vector potential, see [6], Chap. 5.18. The result is

$$\ell \approx \frac{1}{\sqrt{\mu\sigma f}} \tag{37}$$

with σ the conductivity of the conductor. This approximation has to be understood as a rough one which gives only the order of ℓ. As an example we take the conductivity of copper, $\sigma^{-1} = 1,7 \cdot 10^{-8}\,\Omega\text{m}$, and set $f = 10\,\text{GHz}$. This yields $\ell \approx 1,2 \cdot 10^{-6}$ m.

In the following we will use the cut-off scheme since, for an analytical treatment, it is easier to use. Furthermore we will take for a frequency $f = 10\,\text{GHz}$ the cut-off parameter $\varepsilon = \ell = 10^{-6}\text{m}$.

3.5 Explicit evaluation of the first order induced current

It is now instructive to focus on a specific example: Let us set $f = 10\text{GHz}$ (as above), $R = 10\text{cm}$, and $\rho = 1\text{mm}$. This yields, in particular, $k \approx 210\text{m}^{-1}$ and $\kappa = 10\text{m}^{-1}$. Moreover, we have within the curved region of the wire $y' = R\phi'$ and $dy' = R\,d\phi'$. Putting everything together yields

$$\begin{aligned}
&k_{1c}(y=0) = \\
&\rho\kappa \int G'(|y'|)\, k_s(y')|y'|\, dy' = \frac{k_0}{4\pi}\int d\phi' \Big[\\
&\quad -\Big(0.21 \sin(21(|\phi'|+\phi')) + 0.01 \frac{\cos(21(|\phi'|+\phi'))}{|\phi'|}\Big) \\
&\quad +j\Big(0.21 \cos(21(|\phi'|+\phi')) - 0.01 \frac{\sin(21(|\phi'|+\phi'))}{|\phi'|}\Big)\Big] \\
&\qquad =: \frac{k_0}{4\pi}\int \Big(f(\phi') + jg(\phi')\Big)\, d\phi' .
\end{aligned} \tag{38}$$

Let us first investigate the real part $f(\phi')$ of the integrand. It is plotted in Fig. 5.

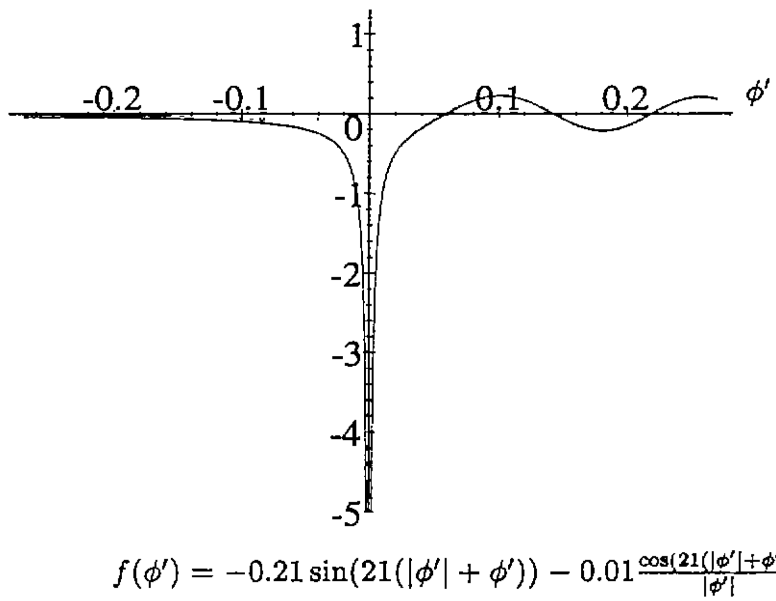

Fig. 5: The real contribution to the integral in (38).

It is immediate to recognize that $f(\phi')$ significantly contributes to the integral only for small values of $|\phi|$. For larger values of ϕ the function $f(\phi')$ is practically sinusoidal and positive and negative contributions cancel out. For negative values of ϕ the arguments of the trigonometric functions of $f(\phi')$ vanish and $f(\phi')$ behaves like $1/\phi'$.

Let us now consider the imaginary part $g(\phi')$ of the integrand which is plotted in Fig. 6.

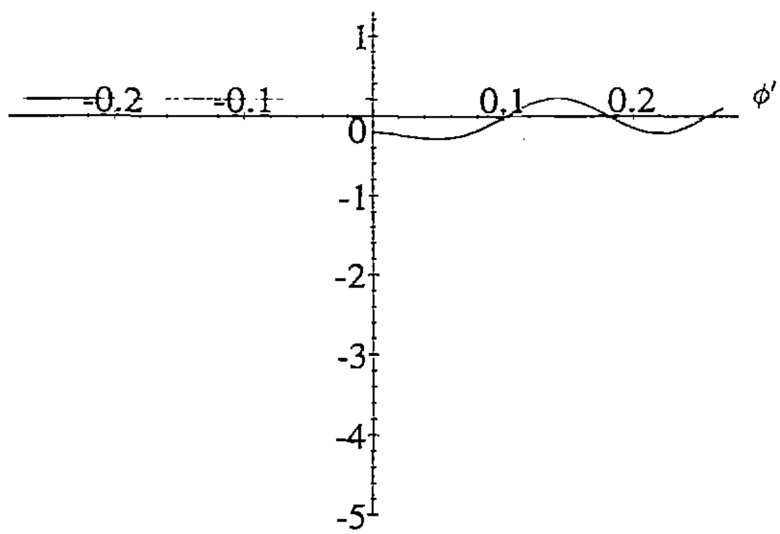

$$g(\phi') = 0.21\cos(21(|\phi'| + \phi')) - 0.01\frac{\sin(21(|\phi'|+\phi'))}{|\phi'|}$$

Fig. 6: The imaginary contribution to the integral in (38).

The function $g(\phi')$ has no singularity at $\phi' = 0$ and does not significantly contribute to the integral around this point. While for positive ϕ' it basically behaves like a cosine, it is a constant for negative ϕ'. This second property is an artifact which is due to our approximation $r' \approx |y'|$. This approximation means that the length of the arc between points y' and y, for $y' < y$, is taken as the linear distance between y' and y such that the travelling wave current is in phase with the electromagnetic field which it emanates at y' and receives at y. This is only true to first order and a more exact calculation leads to a (slow) variation of $g(\phi')$ also for $\phi' < 0$. We should remind us at this point that the curvature expansion was derived under the condition $\kappa y' = \phi' \ll 1$ such that values of $f(\phi'), g(\phi')$ for "large" arguments ϕ' are not meaningful.

The integrals in (38) are quite elementary and can be easily evaluated. Let us define

$$F_+(\Phi) := \int_{10^{-5}}^{\Phi} f(\phi')\,d\phi'\,, \quad F_-(\Phi) := \int_{-\Phi}^{-10^{-5}} f(\phi')\,d\phi'\,,$$
$$G_+(\Phi) := \int_{10^{-5}}^{\Phi} g(\phi')\,d\phi'\,, \quad G_-(\Phi) := \int_{-\Phi}^{-10^{-5}} g(\phi')\,d\phi'\,,$$

with the cut-off parameter $\varepsilon/R = 10^{-5}$. These functions are plotted in Fig.7.

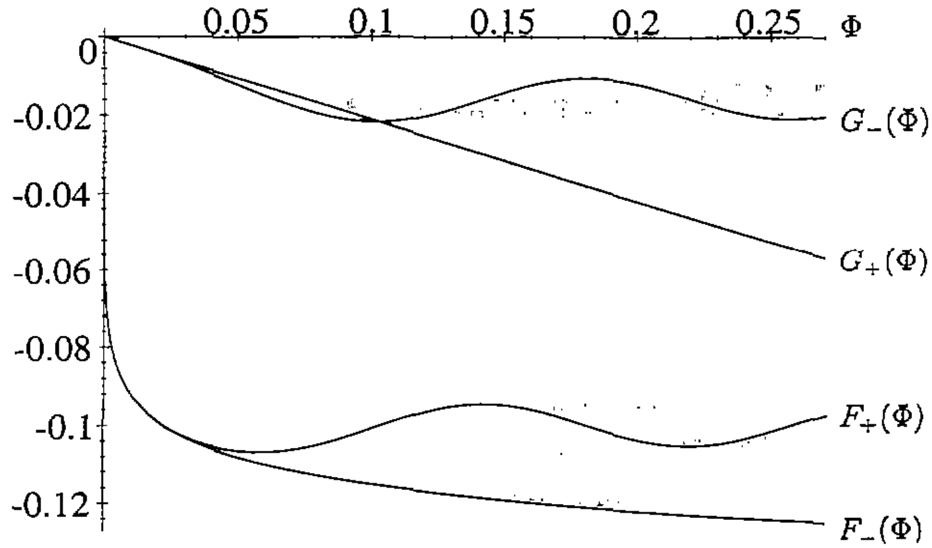

Fig. 7: A plot of the functions F_+, F_-, G_+, and G_- which describe the integrated contributions to the first order induced current k_{1c}.

We qualitatively recognize that the functions F_+, F_- strongly fall off for values $\Phi \lesssim 0.05$ and behave rather stationary for larger values of Φ. Similarly, the function G_+ quickly reaches a stationary value which is less than 20 % of the stationary values of F_+, F_-. Only the function $G_-(\Phi)$ exhibits no stationary behavior for larger values of Φ. As discussed above this is due to the first order approximation $|y'| = r'$.

Let us take as integration limit $\Phi = 0.1$. As is evident from Fig. 7 for this value the dominant functions F_+, F_- become approximatively stationary and the condition $\phi' < \Phi \ll 1$ is fulfilled to a satisfying extent. This value corresponds to an integration domain of length $R\Phi = 1$cm. We then find for the first order induced current

$$\begin{aligned} k_{1c} &= \frac{k_0}{4\pi}\Big(F_+(0.1) + F_-(0.1) + j[G_+(0.1) + G_-(0.1)]\Big) \\ &\approx \frac{k_0}{4\pi}(-0.17 - j0.04) \qquad (39) \\ &\approx -0.02 k_0\, e^{j13.2^\circ} \qquad (40) \end{aligned}$$

In (39) the minus sign in front of the real part indicates that the first order current $\boldsymbol{k}_{1c}$ basically yields a damping of the incoming current wave $\boldsymbol{k}_s$. The imaginary part is responsible for the nontrivial phase factor in (40).

The result (40) is valid for points on the curved part of the wire segment that are at least 1 cm apart from the transition to a straight part of the wire. If a point is closer to such a transition either the upper or lower integration limit has to be adjusted to a corresponding value $\Phi < 0.1$. In this way it is immediate to compute k_{1c} for any point of the curved wire segment. Once this is done it is possible to derive the higher order currents according to

$$k_{(n+1)c}(\boldsymbol{r}) = \rho\kappa \int G'(\boldsymbol{r}, \boldsymbol{r}')\, k_{nc}(\boldsymbol{r}')|y'|\, dy' , \tag{41}$$

compare (33). These integrals, with a function $k_{nc}(\boldsymbol{r}')$ which will usually be different from $k_s(\boldsymbol{r}')$, can be evaluated in the same way as it was just demonstrated for the evaluation of the first order current.

4 Conclusions

With the construction of the induced current on the curved wire segment we have demonstrated that the geometric scattering is a powerful tool for the study of electromagnetic phenomena in the vicinity of curved transmission line structures. Though we started from the basic Maxwell theory it was possible to perform the calculations in a purely analytical manner. The approximations involved were clearly spelled out and can also be used to control the quality of the curvature expansion. There was no need to explicitly calculate radiation integrals for electromagnetic radiation fields in order to describe the current/current interaction on the wire.

The example of the curved wire segment should still be worked out in more detail. These details include the explicit calculation of the higher order induced currents, their explicit dependence on the frequency, the effect of the induced current on the straight parts of the wire segment, and the radiation characteristic at the bend. We will report on these points in a forthcoming paper.

References

[1] C.E. Baum, T.K. Liu, and F.M. Tesche: "On the Analysis of General Multiconductor Transmission-Line Networks", *Interaction Note* **350**, November 1978.

[2] C.E. Baum, J. Nitsch, and R. Sturm: "Analytical Solution for Uniform and Nonuniform Multiconductor Transmission Lines", in *Review of Radio Science* (W.R. Stone, ed.) Oxford: Oxford University Press, 1996, pp. 433-464.

[3] F. Gronwald and J. Nitsch : "A Geometric Scattering Expansion of the Current on Conducting Surfaces and Transmission Line Structures", *Proceedings of the IEEE Symposium on EMC*, held at Seattle, USA, August 1999, (1999); see also *Interaction Note* **555**, June 1999.

[4] C.E. Baum and A.P. Stone: *Transient Lens Synthesis*, (Hemisphere Publishing Corporation, New York, 1991).

[5] M. P. do Carmo: *Differential Geometry of Curves and Surfaces*, 2nd ed., (Prentice Hall, Englewood Cliffs, 1976).

[6] J.D. Jackson: *Classical Electrodynamics*, 3rd edition (John Wiley & Sons, New York, 1998).